Journal of Geosciences and Geomatics, 2022, Vol. 10, No. 1, 65-73
Available online at http://pubs.sciepub.com/jgg/10/1/5
Published by Science and Education Publishing
DOI:10.12691/jgg-10-1-5

Microchemical Fingerprint of Magnetite Bearing Iron Ore Deposit from the Sanaga Prospect, Southern Cameroon: Assessment of Iron Ore-forming Conditions

Bravo Martin Mbang Bonda[1,*], Akumbom Vishiti[1], Mbai Simon Joel[1], Bayiga Elie Constantin[2], Ngon Ngon Gilbert François[2], Etamé Jacques[1,2]

[1]Department of Civil Engineering, University Institute of Technology, University of Douala, P.O.Box 8698, Douala, Cameroon
[2]Department of Earth Sciences, Faculty of Science, University of Douala, P.O. Box 24157, Douala, Cameroon
*Corresponding author: bravobonda@gmail.com

Received March 02, 2022; Revised April 03, 2022; Accepted April 08, 2022

Abstract The Sanaga magnetite bearing iron ore deposit is hosted in the eburnean Nyong complex which constitutes the northwestern edge of the Congo Craton. It is compose predominantly of magnetite bearing quartzite and magnetite-biotite gneisses related to charnockites and amphibole orthogneisses. In this study we use the composition of the magnetite bearing ore to determine their origin and ore formation process. A deposit model is also proposed for a better understanding of the emplacement of the iron ore. EMPA analysis on magnetite reveal variable amount of V, Ti, Al, and Mn. Most of the samples present Ti contents > 0.1%, this indicates a hydrothermal overprint. Although the texture and chemical composition of the magnetite bearing rocks neither represents typical skarn nor BIFs, on Ca + Al + Mn vs Ti + V and Ni + Cr vs Ti + V discrimination diagrams the magnetite reveals a double affinity for skarn and BIF. Elevated contents of Al, Mn and Mg in the magnetite signify crustal contamination while BIF signatures are related to hydrothermal activities. The variable content of V and Ti/V ratio suggests a mixture of reducing and oxidizing environments. On the Al + Mn vs Ti + V binary diagram the magnetite bearing ore reveal hydrothermal temperatures that vary between 200-300°C and 300-500°C. This suggests their precipitation from hydrothermal fluid with medium to high temperature and slight enrichment in Al and Ti. Integrating the data obtained from studies such as regional geology, ore geology and mineral microchemistry, we suggest that the Sanaga magnetite bearing iron ore deposit is similar to the Lake Superior iron ore type and was formed from transgression-regression in back arc basin or continental margin.

Keywords: *magnetite, trace element, hydrothermal alteration, Sanaga prospect, Cameroon*

Cite This Article: Bravo Martin Mbang Bonda, Akumbom Vishiti, Mbai Simon Joel, Bayiga Elie Constantin, Ngon Ngon Gilbert François, and Etamé Jacques, "Microchemical Fingerprint of Magnetite Bearing Iron Ore Deposit from the Sanaga Prospect, Southern Cameroon: Assessment of Iron Ore-forming Conditions." *Journal of Geosciences and Geomatics*, vol. 10, no. 1 (2022): 65-73. doi: 10.12691/jgg-10-1-5.

1. Introduction

Magnetite is a mineral that has been widely used as a petrogenetic indicator [1], it is the most abundant oxide mineral in the earth's crust. It is generally most resistant to alteration and transport than other mineral phases with which it coexists [2]. Moreover, it's an index mineral with a wide range of applications in geophysical studies, igneous petrology and mineral exploration [1,3]. Magnetite have AB_2O_4 as stoichiometric formula, with an average content of trace elements such as Al, Ti, V, Si, Ca, Mn and Mg [4] which can be used to discriminate iron ore types and ore forming processes. The substitution of cations in the different A and B sites probably takes place with low oxygen fugacity; thus Mn, Mg, Zn and Ni can substitute Fe^{2+} while Fe^{3+} can be replaced by Al, V and Cr [5]. Magnetite is an accessory mineral generally found in igneous, metamorphic and sedimentary rocks. It **is** form under variables conditions such as high temperature crystallization in igneous rocks with silicates, sulphur and carbonates magmas or low temperature with hydrothermal fluids. This mineral occurs frequently in hydrothermal magnetite, Fe-Ti-(V) igneous and kiruna deposits. It also occurs commonly in skarn and porphyry Cu deposits. In mineral exploration, one of the toughest challenges is to detect geochemical signatures of proximal and distal deposits of the main mineralization.

In Cameroon several studies have targeted iron ore formations in the southern part of the country. These studies focused on banded iron formation [6-21], magnetite gneisses [22,23,24] and magnetite-martite bearing quartzite [25] with the aim of determining their

origin, age and depositional setting. Iron ore in the Sanaga prospect has been evaluated at 10 million tons (see www.africanmineral.com). Besides [23] that evaluated the chemical composition of magnetite from the Nyong complex, studies which focus on determining the chemical composition of magnetite in Cameroon is rare.

In this study we provide new insight of the chemical composition of magnetite bearing iron ore in the Nyong complex. We present variable textures of magnetite bearing iron ore and their microchemical signatures with the aim to understand their origin and ore-forming processes. A deposit model is also provided for a better understanding of the emplacement of the iron ore.

2. Geological Background

2.1. Regional Geology

The Sanaga magnetite bearing iron ore deposit lies within the Paleoproterozoic Nyong complex, which constitute the northwestern edge of the Archaean Congo Craton in southern Cameroon (Figure 1). The Nyong complex (Figure 1) forms part of the Precambrian geology of Cameroon; it constitutes the main Neoarchaean to Paleoproterozoic complex in Cameroon [23,26,27]. It's a wide band with a NNE-SSW orientation and is composed mainly of migmatitic gneisses [28,31]. It is a well preserved rock unit of the West Central African Belt (WCAB), situated on the Eburnean layer of the Congo Craton.

Lithologically, the Nyong complex is composed of charnockites, gneisses with composition of TTG, mafic-ultramafic rocks are expressed by pyroxenites and amphibolites; meta quartzites, Banded Iron Formation, granodiorite, syenites and augen diorites. Genetically, the Nyong complex is attributed to a proximal domain characterized by the remobilization of the Archaean adjacent cratonic crust [30]. According to [27], the Nyong complex is characterized by a flat S1/S2 foliation, locally open folds and stretching lineation, all associated with N-S sinistral strike slip faults in the western edge [23,28,31,32]. According to [26] the Nyong complex has experienced poly-phase deformation with a granulite-amphibolite facies metamorphism attained in the eburnean.

2.2. Local Geology Deposit

The Sanaga prospect (Figure 2) is composed predominantly of charnockitic gneisses, amphibole bearing orthogneisses**,** magnetite-biotite gneisses that dips 10° to the NE and magnetite-martite bearing quartzite situated at the southern slope of the Mangombe hill, in the center of the studied area. The magnetite-martite bearing quartzite is oriented NE-SW evidence of an eburnean fingerprint. It is constituted of faults in the eastern and western parts that form a corridor between which exist a horst called Mangombè hill.

2.3. Magnetite-martite Bearing Quartzite

The magnetite-martite bearing quartzite is the main iron ore formation in this area. It is subdivided into two facies: banded and massive [25]. Both facies presents a succession of discontinuous quartz rich and magnetite-martite rich bands. Magnetite + quartz + pyroxene + martite ± amphibole ± biotite ± apatite is the main mineral assemblage. Magnetite varies from irregular crystals in the magnetite rich band to crystals associated with pyroxene in bands rich in quartz and isolated magnetite grain [25]. Their whole rock geochemistry shows that the magnetite-martite bearing quartzite has a sedimentary origin. According to [25] the magnetite- martite bearing quartzite may have undergone a significant input from hydrothermal sources with fingerprints of the clastics materials during their deposition.

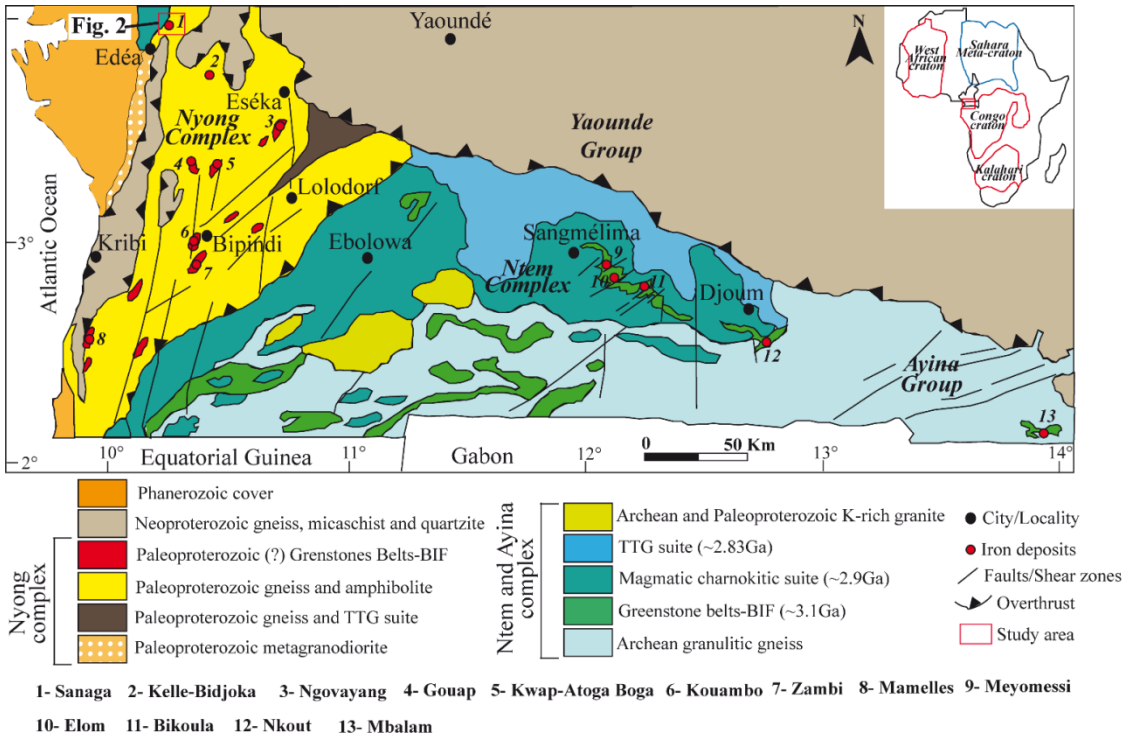

Figure 1. Geological sketch map of southern Cameroon showing the location of the Sanaga iron ore deposits (Figure 2, adapted after [33] and [34])

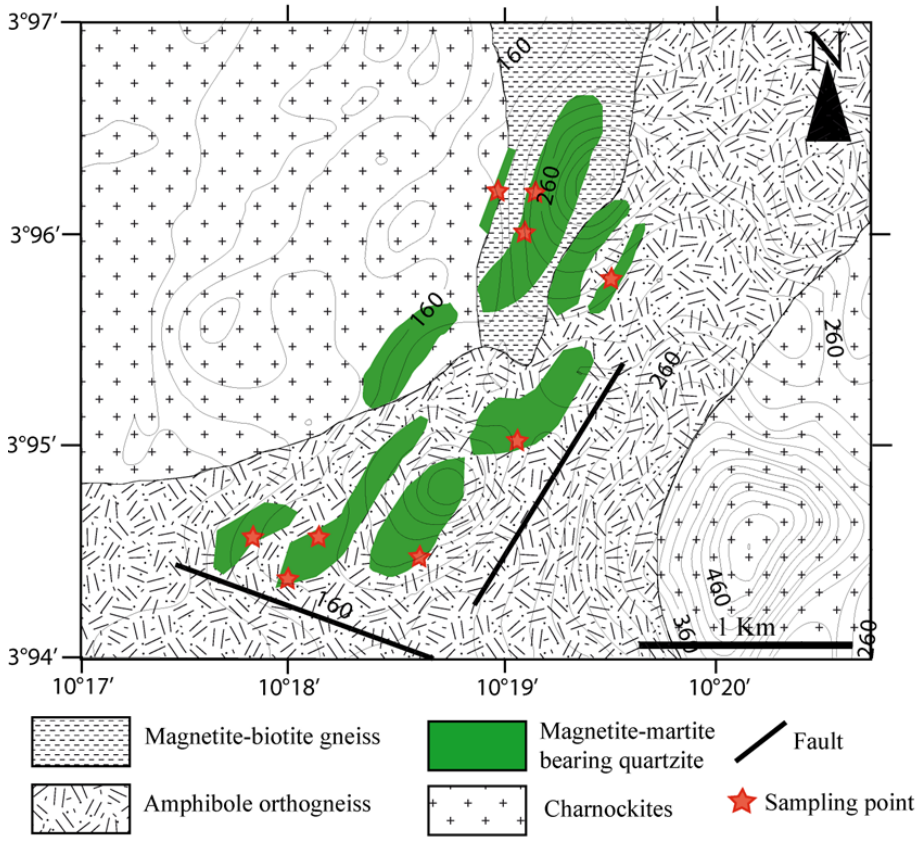

Figure 2. Geological sketch map of the Sanaga prospect (modified after CMC, see www.africanmineral.com)

3. Sampling and Analytical Techniques

In this study, a total of eleven (11) representative samples of magnetite bearing ore were used for mineralogical and microchemical analysis at the petrology and mineralogy laboratory of the Department of Geosciences, University of Padova, Italy. Samples used for polished thin sections were cut using a rock cutter, to rectangular cubes (4×2.5×1 cm) and placed on a glass slide using araldite gum. It was then polished down to 0.3 mm. The mineralogical composition of the samples was determined using a petrographic microscope in transmitted and reflected light.

Their microchemical signature was realized with a CAMECA SX-100 Electron Probe Micro-Analyzer using a 1 µm spot size with acceleration voltage of 15 kV, and a beam current of 20 nA. Magnetite crystals were targeted to determine major and trace elements such as Mg, Al, Si, Ca, Ti, V, Cr, Mn, Fe, Co, Ni and Zn. The detection limit for major elements was set at 0.01% and 0.001 ppm for trace elements. Standards used include Si4+, Mg^{2+}, Ti^{4+}, Fe^{2+}, Al^{3+}, Mn^{2+}, Zn^{2+}, Ni^{2+}, Cr^{2+}, O^{2+}, V^{3+}, Ca^{2+},Co^{2+}, for O, MgO new for Mg, Al_2O_3-20 for Al, Woll-20 for Si, Diopside-20 for Ca, $MnTiO_3$-20 for Ti, Vanadium for V, Cr_2O_3-20 for Cr, $MnTiO_3$-20 for Mn, Fe_2O_3-20 for Fe, Co for Co, NiO-20 for Ni and Blende (ZnS) for Zn.

4. Analytical Results

4.1. Petrography and Mineral Composition

Magnetite in the Sanaga iron ore prospect is hosted by magnetite martite bearing quartzite and magnetite-biotite gneiss. The petrography and mineralogical composition of the magnetite martite bearing quartzite is presented in [25]. Two facies have been determined: the massive and the banded facies.

4.2. Magnetite Biotite-gneiss

The magnetite-biotite gneisses show a characteristic augen texture with tiny bands of magnetite (Figure 3a). The gneisses present mylonitic shistosity with preferential oriented sigmoidal feldspar. It is mainly composed of microcline, biotite, quartz, pyroxene, plagioclase, aegerine-augite and magnetite (Figure 3b). Quartz, microcline and plagioclase show euhedral crystals and occur as disseminations. Plagioclase reveals a characteristic twin while magnetite occurs disseminated or as inclusions in biotite and aegerine-augite. Biotite also defines the rims of plagioclase and K-feldspars.

4.3. Mineral Microchemistry

4.3.1. Magnetite-martite Bearing Quartzite

The microchemical composition of magnetite from the magnetite-martite bearing quartzite is summarized in Table 1. The magnetite show $Fe_2O_3^T$ contents between 92 and 94 wt.%. Besides $Fe_2O_3^T$ it is enriched in TiO_2, Al_2O_3, MgO and MnO. However the massive facie shows higher concentrations of TiO_2, MgO and MnO compared to the banded facie (Table 1). The concentration of others major oxides are relatively low. Cr_2O_3 show values that range from 0 to 0.04 wt.%; V_2O_3 varies between 0 and 0.083 wt.%. The concentrations of CoO and NiO are generally less than 0.017 wt.%. The samples show low

concentrations of trace elements such as Co, Ni, Zn, Cr, V, Ti and Al. On binary plots the massive and banded facies of the magnetite bearing ore shows a positive correlation between Ti and Al; Al and Si (Figure 4).

4.3.2. Magnetite-biotite gneiss

The composition of magnetite from the magnetite-biotite gneiss is presented in Table 2. The concentration of $Fe_2O_3^T$ in the magnetite varies between 91.26 and 94.45 wt%. Concentrations of SiO_2 (0.01-0.07 wt.%); Al_2O_3 (0-0.09 wt.%); V_2O_3 (0-0.08 wt.%); Cr_2O_3 (0-0.03 wt.%) and NiO (0-0.01 wt.%) are low while the content of CaO in the samples reach a maximum of 0.03wt%. On binary plots (Figure 4) the magnetite-biotite gneiss shows a positive correlation between Ti and Al as well as Al and Si (Figure 4). On continental crust normalized trace element diagrams after [35], the magnetite presents similar spider patterns, with depletion in Si, Al, Ca, and enrichment in Mn, Mg, Ti, Zn, V, Ni and Cr (Figure 5). They are also enriched in Mn, Mg, Ti, Ni and Cr compared to the continental crust.

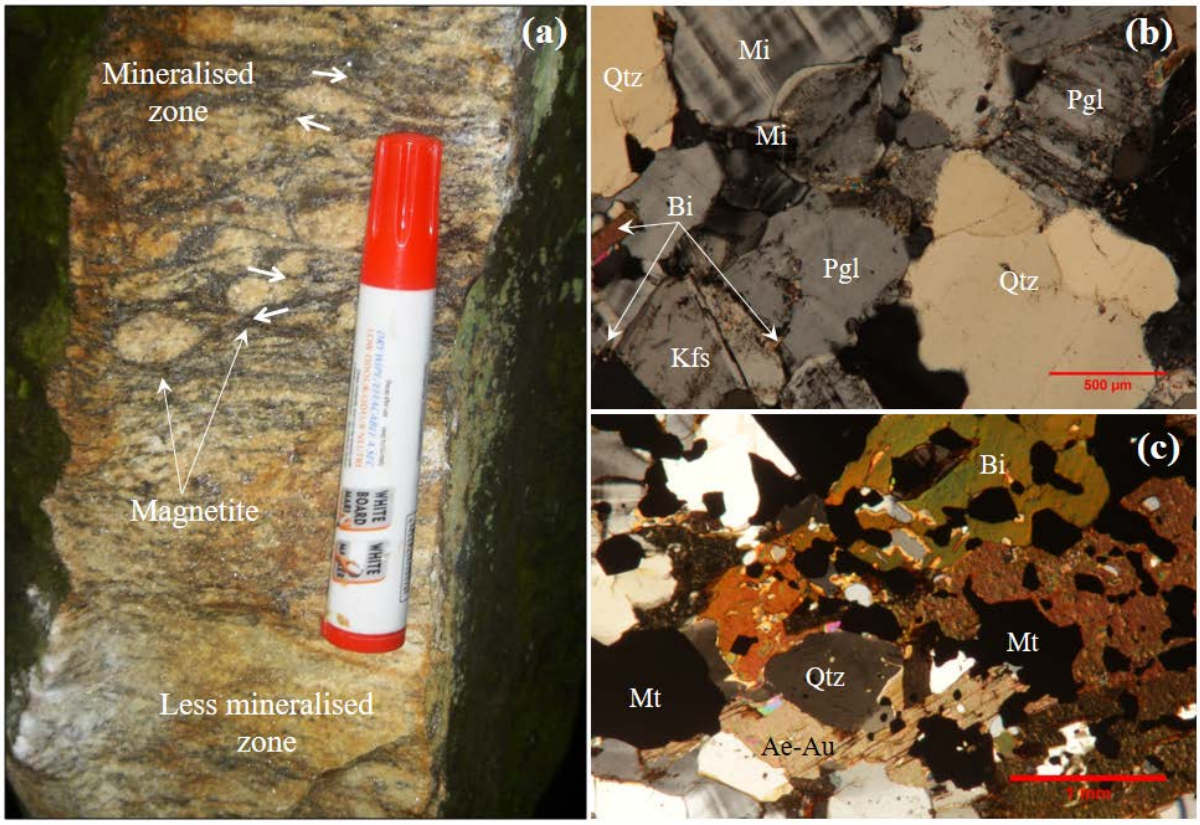

Figure 3. (a) Representative sample and photomicrographs of the magnetite-biotite gneiss showing texture, deformation and distribution of minerals in the rocks. White arrows presents shear orientation. Notice the augen texture. (b)-(c) Transmitted light photomicrographs showing the mineralogical composition of the magnetite-biotite gneiss. Qtz; quartz, Mi: microcline, Bi: biotite, Pgl: plagioclase, Kfs: potassic feldspar, Mt: magnetite, Ae-Au: aegerine - augite

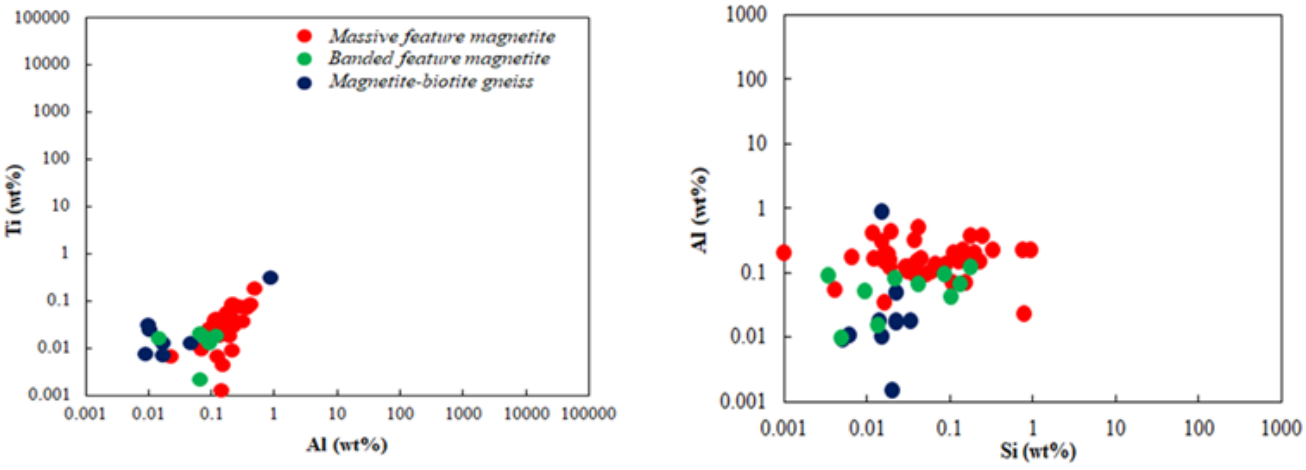

Figure 4. Binary plots showing the variation between Ti vs Al and Al vs Si in magnetite from the Savage prospect

Table 1. EPMA results for major and some trace elements in magnetite from magnetite-martite quartzite

Deposit	Sanaga iron deposit																									
	Massive facies																Banded facies									
Sample	Cmr01								Cmr02				Cmr03				EDN01				EDN03				EDN04	
	1	2	3	4	5	6	7	8	9	10	11	12	13	14	15	16	17	18	19	20	21	22	23	24	25	26
SiO_2*(wt%)*	0.01	0.04	0.04	0	0.04	0.04	0.03	0.03	0.04	0.71	0.03	0.04	0.04	0.08	0.09	0.04	0.03	0.02	0.01	0.09	0.05	0.18	0.01	0.22	0.29	0.38
TiO_2	0.04	0.07	0.13	0.07	0.09	0.06	0.07	0.13	0.08	0.05	0.12	0.09	0.05	0.06	0.29	0.07	0.03	0	0	0	0.03	0.02	0	0	0.03	0.03
Al_2O_3	0.33	0.22	0.81	0.37	0.35	0.3	0.32	0.76	0.38	0.43	0.56	0.33	0.27	0.6	0.95	0.36	0.03	0.1	0.17	0.13	0.15	0.18	0.02	0.08	0.13	0.23
Cr_2O_3	0	0	0	0.02	0	0.04	0.02	0.01	0	0.01	0.02	0.02	0.02	0.02	0	0	0	0	0	0	0	0	0.03	0	0	0.03
$Fe_2O_3^T$	92.47	93.1	91.3	92.4	93.1	92.45	92.3	92.68	91.5	90.84	92.06	91.65	92.27	91.64	91.4	91.7	0	0	0.01	0.03	0	0	0	0	0.01	0.02
MnO	0.08	0.04	0.08	0.06	0.1	0.09	0.03	0.08	0.11	0.07	0.11	0.1	0.07	0.08	0.14	0.08	91.59	92.67	92.31	89.9	89.83	88.7	92.16	89.3	87.75	89.03
MgO	0.13	0.16	0.27	0.13	0.18	0.19	0.13	0.26	0.23	0.15	0.2	0.22	0.18	0.16	0.3	0.2	0.05	0.06	0.01	0.07	0.02	0.08	0.04	0.1	0.02	0.01
V_2O_3	0.02	0.01	0	0	0	0.02	0.02	0	0.01	0.04	0.01	0	0	0.04	0.02	0.02	0.36	0.32	0.37	0.27	0.38	0.35	0.35	0.33	0.42	0.33
CaO	0	0	0	0	0	0.01	0.01	0	0	0	0	0.01	0	0.01	0	0.01	0.01	0	0	0	0	0.03	0	0.01	0.02	0.02
NiO	0.02	0.01	0	0	0.01	0	0.03	0	0.04	0	0	0	0	0.02	0.07	0.03	0.04	0	0	0	0.02	0	0.01	0	0.02	0.02
ZnO	0	0.02	0	0	0	0	0	0	0	0.02	0.05	0.09	0	0	0.01	0.04	0	0	0.14	0.07	0	0	0	0	0	0
Si*(ppm)*	66	187	194	10	166	189	124	118	170	3325	152	182	166	377	428	183	139	97	35	426	218	862	49	1048	1332	1795
Ti	223	401	800	398	523	332	448	760	461	290	726	543	324	355	1724	428	157	0	3	21	165	124	3	0	202	181
Al	1750	1184	4307	1968	1873	1572	1677	4038	2029	2277	2942	1757	1452	3163	5050	1895	151	523	904	672	791	933	97	417	664	1203
Cr	11	0	11	168	0	311	157	112	0	45	146	123	156	157	0	0	22	34	0	0	22	0	236	0	0	262
Mn	637	283	596	479	812	697	221	616	819	521	877	766	560	637	1121	653	351	436	47	529	137	648	342	736	150	97
Mg	787	964	1621	804	1085	1132	804	1591	1382	910	1228	1344	1061	953	1830	1199	2156	1938	2247	1604	2263	2127	2085	2013	2505	1978
V	108	77	16	0	0	138	108	0	77	248	93	0	0	263	124	108	0	0	47	186	0	16	0	0	93	142
Ca	0	0	15	0	29	97	43	0	0	0	29	36	0	83	0	40	95	0	0	33	22	178	0	51	160	114
Ni	167	78	0	0	56	0	223	0	346	0	0	0	0	156	534	234	325	0	0	11	134	0	56	0	123	193
Zn	0	155	0	0	0	0	0	0	0	155	379	714	0	0	112	351	28	0	1102	550	0	0	0	0	0	0

Table 2. EPMA results for major and trace elements in magnetite from the magnetite-biotite gneiss

Deposit	Sanaga iron deposit													
Sample	EDN06								EDN07					
	1	2	3	4	5	6	7	8	9	10	11	12	13	14
SiO_2*(wt%)*	0.04	0.03	0.01	0.03	0.02	0.01	0.07	0.07	0.05	0.05	0.03	0.04	0.05	0.07
TiO_2	0.04	0.02	0.01	0.05	0.00	0.04	0.04	0.02	0.00	0.00	0.01	0.00	0.02	0.03
Al_2O_3	0.00	0.00	0.02	0.02	0.00	0.02	0.00	0.03	0.03	0.03	0.03	0.00	0.09	0.00
Cr_2O_3	0.01	0.01	0.00	0.00	0.02	0.00	0.01	0.00	0.00	0.00	0.03	0.02	0.01	0.03
$Fe_2O_3^T$	93.51	94.04	93.20	93.41	91.26	92.25	93.33	93.40	94.45	93.76	93.62	92.60	93.64	93.39
MnO	0.09	0.05	0.07	0.00	0.04	0.03	0.05	0.03	0.05	0.02	0.06	0.06	0.05	0.04
MgO	0.11	0.11	0.15	0.10	0.15	0.10	0.15	0.09	0.11	0.18	0.12	0.10	0.12	0.10
V_2O_3	0.05	0.08	0.01	0.03	0.04	0.06	0.00	0.02	0.04	0.05	0.03	0.06	0.02	0.04
CaO	0.00	0.01	0.00	0.01	0.03	0.00	0.00	0.00	0.01	0.00	0.00	0.00	0.02	0.03
NiO	0.04	0.00	0.01	0.03	0.00	0.09	0.05	0.00	0.02	0.03	0.00	0.00	0.04	0.04
Si *(ppm)*	188	136	52	155	116	62	323	345	231	231	142	206	230	312
Ti	233	136	73	294	0	235	226	127	3	0	70	3	127	205
Al	0	0	93	102	0	108	0	173	180	166	176	15	475	0
Cr	79	68	23	0	143	0	102	0	34	22	202	122	101	213
Mn	674	406	528	0	342	203	417	240	362	161	471	500	390	278
Mg	665	634	899	597	915	631	875	573	682	1066	732	584	694	593
V	358	561	62	221	274	434	0	140	282	340	233	430	125	279
Ca	0	87	0	103	225	0	0	0	88	0	0	25	117	217
Ni	281	0	45	227	0	738	431	0	125	201	0	0	281	279
Zn	0	85	43	0	0	437	458	184	86	112	0	14	71	465

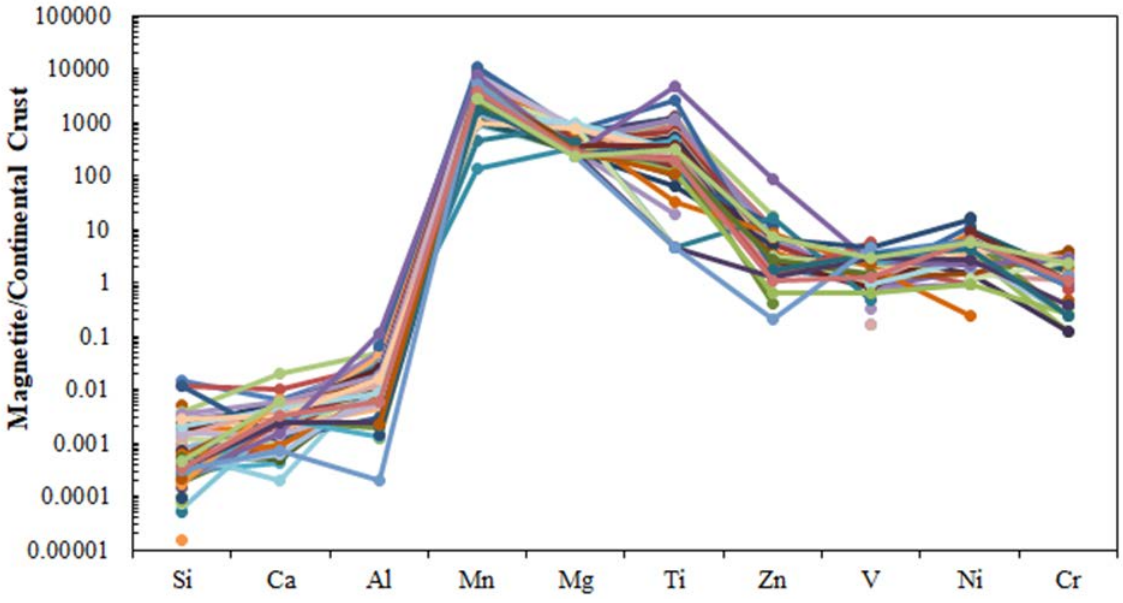

Figure 5. Spider diagram of magnetite composition from the Sanaga iron ore prospect

5. Discussion

5.1. Fingerprinting Hydrothermal Process Using Microchemistry

Numerous studies have focused on the chemical composition of magnetite ore around the world [1,3,4,35,36,37]. Trace element behavior in magnetite has been used as a tool for petrogenetic studies and the determination of provenance [36]. On the Ti vs Ni/Cr diagram after [37] and/or [38], magnetite can be classified as hydrothermal or magmatic in origin. If the magnetite has a hydrothermal affinity the Ni/(Cr + Mn) vs Ti + V or (Ca + Al + Mn) vs Ti + V diagrams after [3] can be used to differentiate its signature. It has been modified, by [1] to differentiate magnetite into IOCG, Skarn, BIF, Fe-Ti, Kiruna and Porphyry types. If the magnetite shows a magmatic affinity, then the MgO/(MgO + Al_2O_3) diagram after [39] can be used to differentiate the rock into felsic, mafic and intermediate domain.

The studied magnetite ore have a chemical composition characterized by enrichment in Si, Al, Fe, Mn, Mg, V, Ca and Ti. According to [3] and [1] Ti and Cr are incompatible elements in magnetite during hydrothermal alteration. Magnetite with hydrothermal and BIF affinities have Ti< 2%; moreover, magnetite with typical BIF affinity have Ti < 0.1%. The magnetite in this study show Ti > 0.1%, this suggests a hydrothermal signature. Furthermore, on the Ti versus Al discrimination diagram of [38] magnetite shows a hydrothermal (Figure 6) signature. However, discrimination diagrams after [3] reveals both skarn and BIF affinities (Figure 7) for the magnetite. This can be related to the behavior of Al in hydrothermal process. In this study, the massive facies is Al-rich compared to the banded facies; so Al, Si and Ca are incompatible elements in magnetite. Hydrothermal skarn is enriched in Mg, Al, Mn, Co, Ni and Zn [1]. We have shown that magnetite in the study area is enriched in Mg, Mn and Al with minor amounts of Cr, Co, Ni and Zn. This suggest that magnetite from the Sanage prospect is not skarn in origin. The high content of Al, Mn, and Mg in the magnetite suggests crustal contamination.

Although the magnetite show BIF signatures their texture and chemistry differs from that of typical BIF. BIFs are characterized by regular alternating and continuous bands, a negative Ce and positive Eu anomalies. According to [25] the magnetite- martite bearing quartzite shows irregular discontinuous alternating bands. They lack a positive Eu and negative Ce anomalies. This therefore excludes the BIF setting [23]. BIF signature presented by the magnetite can be attributed to hydrothermal activity at temperatures < 500°C.

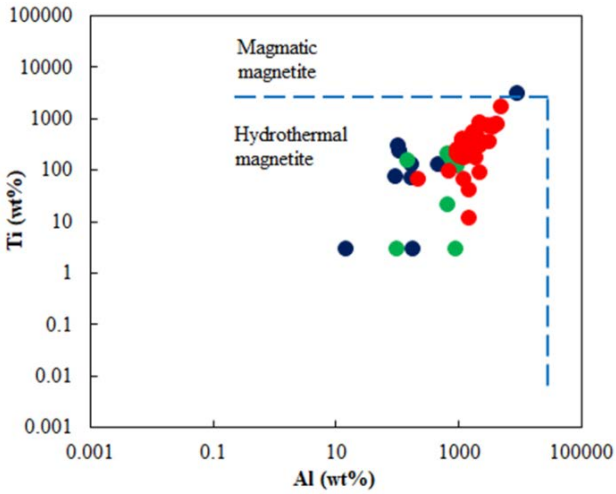

Figure 6. Ti vs Al plot after [38] of magnetite from the Sanaga prospect

5.2. Ore-forming Conditions

Hydrothermal magnetite has several factors that controls their formation such as: temperature, pressure, fluids composition, oxygen fugacity, host rock composition or coexists minerals [1,40]. In natural fluids, V can be present as V^{3+}, V^{4+} and V^{5+}. Oxygen fugacity (*f*O2) may control the V content in magnetite. Moreover, only V^{3+} can be highly partitioned into magnetite. [1] indicate that

V can be enriched in magnetite formed from reducing fluids. Magnetite formed in reducing fluids has lower Ti/V ratios relative to those in oxidizing fluids [40]. The magnetite bearing ore from the Sanaga prospect show high concentrations of V in the magnetite-biotite gneiss compared to the magnetite-martite bearing quartzite. Ti/V ratios for biotite gneisses are low (range between 0.0069-1.33), only one sample shows a high ratio (12.28). Thus the magnetite from the magnetite-biotite gneisses was formed under reducing conditions. Ti/V ratios calculated for magnetite-martite bearing quartzite are variables in the massive facie. Ratios range between 0.38 and 9.06 for the massive facie while the banded facie reveals ratios that vary from 0.06 to 2.17. This suggests that the magnetite-martite bearing quartzite was formed in an environment with both reducing and oxidizing conditions.

Temperature may have an influence on few elementals contents in magnetite, such as Mg, V, Ti and Al. Incorporation of these elements in magnetite is evident in magmatic systems with high temperatures, but they are immobile in low-temperature hydrothermal fluids [41].

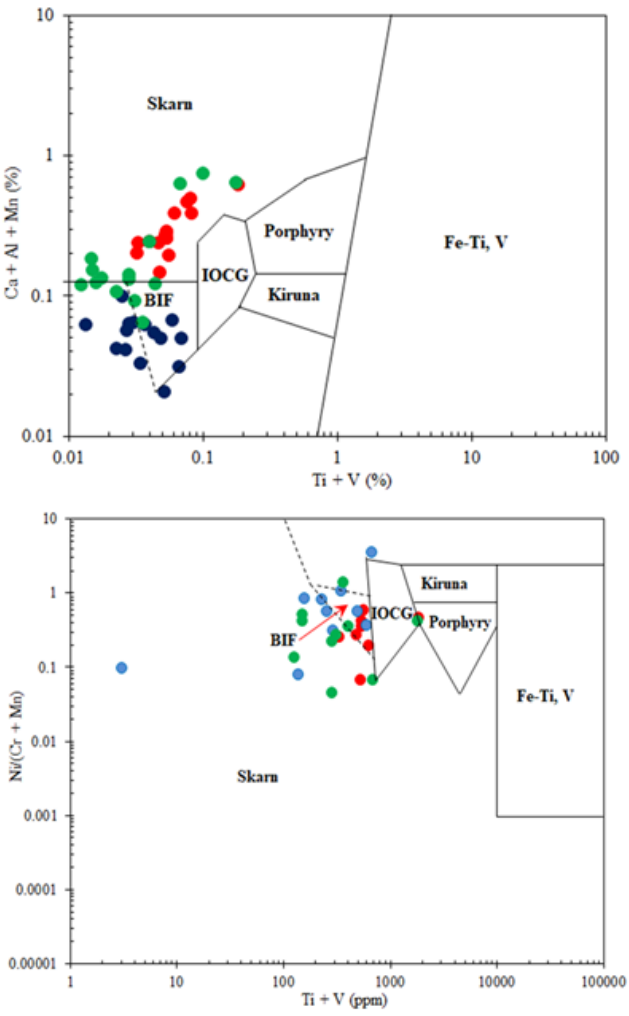

Figure 7. Binary Ca+Al+Mn vs Ti+V and Ni/Cr vs Ti+V plots (adapted from [39]) of magnetite from Sanaga propect

High contents of Al, V, Ti and Mn in magnetite suggest that magnetite samples are related to volcanic rocks [40]. Magnetite from the magnetite-martite bearing quartzite and biotite gneiss show variable content of Al, V, Ti and Mn in the (Al + Mn) vs (Ti + V) diagram that discriminates the formation temperatures of magnetite [1]. Most of the samples from the magnetite-martite bearing quartzite and biotite gneiss plot in the 200-300°C field while few sample plot in the 300-500°C field (Figure 8). This suggests that magnetite in the Sanaga prospect was precipitated from medium to high temperature fluids slightly enriched in Al and Ti. The slight enrichment in Al + Mn and Ti + V also suggests that the magnetite-martite bearing quartzite is not from a volcanic origin. According to [1], coexisting silicates and sulfides phases have an important compositional control in hydrothermal magnetite. Silica and sulfide minerals preferentially incorporate chalcophile and lithophile elements respectively [1,40]. The Sanaga magnetite iron ore is particularly composed of magnetite, without sulfides and variable amount of silicates (quartz and pyroxene). The studied magnetite indicates low concentrations of Ti, V and Cr thus the presence of the silicate phase did not affect their concentration in the hydrothermal magnetite. This situation may explain that minor amount of silicates phases in the magnetite-martite bearing quartzite did not affect the composition of magnetite during hydrothermal process.

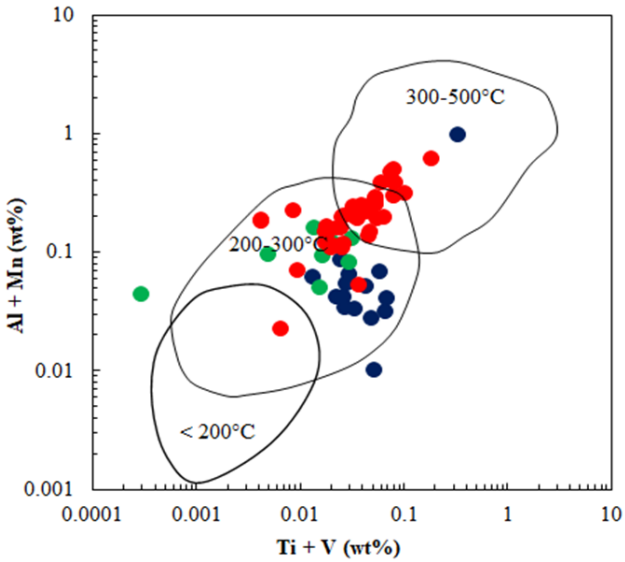

Figure 8. Plot of Al + Mn vs. Ti + V for different formation temperatures of magnetite. References fields are adapted from [1]

5.3. Ore Deposit Model

Recently, [25] and [42] showed that the Sanaga iron ore are formations with sedimentary origin. They are different from BIF by lack of Ce anomaly and textural evidence. Therefore, they are related to rocks of the Nyong complex which represent the NW edge of the Congo Craton. Compared to the Algoma type, the magnetite-martite bearing quartzite have low amount of transition metals such as Ni (mean 24.8 ppm), Co (mean 4.3 ppm) and V (mean 20.5 ppm) (see [25]). This suggests that the Sanaga iron ore are not volcanic in origin. These values are similar to those of Lake superior iron formation reported by [43] (32 ppm; 27 ppm; 30 ppm respectively). Moreover the Sanaga iron ore is situated at the edge of the Congo Craton. We can therefore suggest that the mode of formation of the Sanaga iron ore deposit is similar to that of the Lake superior type. However, [44] reported that

rocks formed in a rift context or residual sea is enriched in LREE because these environments are close to the continent. The magnetite-martite bearing quartzite presents enrichment in LREE (see [25]) with signatures of crustal contamination. Moreover all discriminating diagrams show that these magnetite-martite bearing quartzites are formed by hydrothermal activity. Thus we suggest that the Sanaga iron ore was deposited in continental margin or back arc basin like the Lake superior iron formations by transgression-regression phenomenon with a combination of three process: (1) hydrothermal solutions and fluvial activity from which Fe, Si and REE precipitated; (2) terrigenous sedimentation; (3) oxidation, producer of iron formation (Figure 9).

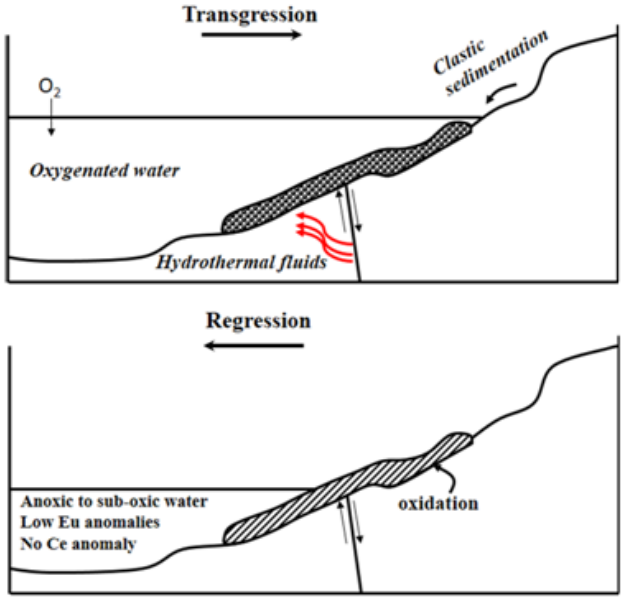

Figure 9. Schematic Deposit model of magnetite quartzite from Sanaga iron deposit

6. Conclusions

The main conclusions from this work are as follows:

1) The magnetite martite bearing quartzite and the magnetite-biotite gneiss are the main sources of magnetite in the Sanaga prospect.

2) Magnetite from the study area show a hydrothermal signature on discrimination diagrams. This is supported by Ti contents > 0.1 %.

3) Although the magnetite show signatures of skarn and BIF on discrimination diagrams, they lack characteristic signatures of skarn. High contents of Al, Mn and Mg in the magnetite can be attributed to crustal contamination. The magnetite martite bearing quartzite lacks characteristic textures and chemical signatures of BIF. Their BIF signature can be related to hydrothermal activities at temperatures < 500°C.

4) The behavior of V and Ti/V ratio calculated suggest a mixture of reducing and oxidizing environment for the magnetite. Furthermore, magnetite grains on Al + Mn vs Ti + V diagrams show moderate to high temperatures with a slight enrichment in Al and Ti.

5) Sanaga iron deposit have a minor amount of transition metals such as Ni, Co and V suggesting that they are not related to volcanic rocks but similar to Lake Superior iron formation type. Ore deposition took place in continental passive margin or back arc basin by transgression-regression.

Acknowledgements

We are grateful to Prof. Paolo Nimis and Prof Claudio Mazzoli of the Department of Geosciences, University of Padova, Italy for their availability and assistance in the acquisition of the EMPA data. We are also gratefully to anonymous reviewer and the Editor Chief whose comments improved on the quality of this work.

References

[1] Nadoll, P., Angerer, T., Mauk, J.L., French, D., Walshe, J., The chemistry of hydrothermal magnetite: a review, *Ore Geology Review*, 2014, 61, 1-32.

[2] McClenaghan, M.B., Indicator mineral methods in mineral exploration. *Geochemical Exploration Environmental Analysis* 5, 2005, 233-245.

[3] Dupuis, C., Beaudoin, G., Discriminant diagrams for iron oxide trace element fingerprinting of mineral deposit types. *Mineral. Deposita 46*, 2011, 319-335.

[4] Nadoll, P., Mauk, J.L., Hayes, T.S., Koenig, A.E., Box, S.E., Geochemistry of magnetitefrom hydrothermal ore deposits and host rocks of the Mesoproterozoic BeltSupergroup, *United States Economic Geology* 107 (6), 2012, 1275-1292.

[5] Lindsley, D.H., 1991. Oxide minerals: petrologic and magnetic significance, *Review Mineralogy, Mineralogy Society American* 25, 509.

[6] Suh, C. E., Cabral, A. R., Shemang, E. M., Mbinkar, L. and Mboudou, G. G., M., Two contrasting iron-ore deposits in the Precambrian mineral belt of Cameronn, West Africa. *Exploration and Mining Geology* 17, 2008, 197-207.

[7] Suh, C. E., Cabral, A., Ndime, E. N., Geology and ore fabrics of the Nkout high grade haematite deposit, southern Cameroon. *Smart Science Exploration Mineral* 1, 2009, 558-560.

[8] Chombong, N.N. and Suh, C.E., 2883 Ma commencement of BIF deposition at the Northern edge of Congo Craton, Southern Cameroon: New zircon SHRIMP data constraint from metavolcanics, *Episodes*, *36*, 2013, 47-57.

[9] Ilouga, C., Suh, C.E., Tanwi, G.R., Textures and Rare Earth Elements Composition of Banded Iron Formations (BIF) at Njweng Prospect, Mbalam Iron Ore District, Southern Cameroon. *International Journal of Geosciences* 4, 2013, 146-165.

[10] Ilouga D. C. I., Ndong Bidzang F., Ziem A Bidias L. A., Olinga J. B., Tata E., Minyem D., Geochemical Characterization of a Stratigraphic Log Bearing Iron Ore in the Sanaga Prospect, Upper Nyong Unit of Ntem Complex, Cameroon, *Journal of Geosciences and Geomatics*, vol 5, 2017, 218-228

[11] Kelvin, F.E.A., Wall, F., Gavyn, K.R. and Moon, C.J., Quantitative mineralogical and chemical assessment of the Nkout iron ore deposit, southern Cameroon. *Ore Geology Reviews*, 64, 2014, 25-39.

[12] Ganno, S., Ngnotue, T., Kouankap, N.G.D., Nzenti, J.P., Notsa, F.M., Petrology and geochemistry of the banded iron-formations from Ntem complex greenstones belt, Elom area, Southern Cameroon: Implications for the origin and depositional environment. *Chemie der Erde* 75, 2015, 375-387.

[13] Ganno, S., Moudioh, C., Nzina Nchare, A., Kouankap Nono, G.D. and Nzenti, J.P., Geochemical Fingerprint and Iron Ore Potential of the Siliceous Itabirite from Palaeoproterozoic Nyong Series, Zambi Area, Southwestern Cameroon. *Resource Geology*, 66, 2015, 71-80.

[14] Ganno S., Njiosseu, T.E.L., Kouankap, N.G.D., Djoukouo, S.A., Moudioh C., Ngnotué T., Nzenti J.P., A mixed seawater and hydrothermal origin of superior-type banded iron formation (BIF)-hosted Kouambo iron deposit, Palaeoproterozoic Nyong series,

Southwestern Cameroon: Constraints from petrography and geochemistry. *Ore Geology Reviews* 80, 2017, 860-875.

[15] Anderson, K. F. E., Frances, W., Rollinson G. K., Charles J. M., Quantitative mineralogical and chemical assessment of the Nkout Iron ore deposit, southern Cameroon. *Ore Geology Reviews* 62, 2014, 25-39.

[16] Ndime E. N., Ganno, S., Soh, T. L., Nzenti, J. P., Petrography, lithostratigraphy and major element geochemistry of Meso-archean metamorphosed banded iron formation-hosted Nkout iron ore deposit, north western Congo Craton, Central West Africa. *Journal of Earth Sciences* 148, 2018, 80-98.

[17] Ndime, E. N., Ganno, S., Nzenti, J. P., Geochemistry and Pb-Pb geochronology of the Neoarchean Nkout West metamorphosed banded iron formation, Southern Cameroon. *International Journal of Earth Sciences* 108, 2019, 1551-1570.

[18] Soh, T. L., Nzepang, T. M., Chongtao, W., Ganno, S., Ngnotued, T., Kouankap, N. G. D., Shaamu, J. S., Zhang, J., Nzenti, J. P., Geology and geochemical constrains on the origin and depositional setting of the Kpwa-Atog Boga banded iron formations (BIFs), northwestern Congo Craton, southern Cameroon. *Ores Geology Reviews*, 95, 2018, 620-638.

[19] Tchatchueng, R., Ngnotué, T., Njiosseu, E.L.T., Ganno, S., Wabo, H. and Nzenti, J.P, Contrasting Depositional Environment of Iron Formation at Endengue Area, NW Congo Craton, Southern Cameroon: New Insights from Trace and Rare Earth Elements Geochemistry. *International Journal of Geosciences*, 12, 2021, 280-306.

[20] Ndema M.J.L. and Aroke E.A., Petrology and Geochemical Constraints on the Origin of Banded Iron Formation-Hosted Iron Mineralization from the Paleoproterozoic Nyong Serie (Congo Craton, South Cameroon), Pout Njouma Area (Edea North): Evidence for Iron Ore Deposits. *International Journal of Research and Innovation in Applied Science*, 5, 2020, 19 p.

[21] Soh Tamehe, L., Chongtao, W., Ganno, S., Jeremia Simon, S., Kouankap Nono, G.D., Nzenti, J.P., Lemdjou, Y.B., and Htun Lin, N., Geology of the Gouap iron deposit, Congo Craton, southern Cameroon: Implications for iron ore exploration: *Ore Geology Reviews*, v. 107, 2019, 1097-1128.

[22] N.N. Chombong, E.C. Suh, C.D.C. Ilouga, New detrital zircon U-Pb ages from BIF-related metasediments in the Ntem complex (Congo Craton) of southern Cameroon, West Africa, *Natural science* 5, 2013, 835-847.

[23] Chombong, N. N., Suh C. E., Lehmann B., Vishiti A., Ilouga D. C., Shemang E. M., Tantoh B. S. and A. C. Kedia. Host rock geochemistry, texture and chemical composition of magnetite in iron ore in the Neoarchaean Nyong unit in southern Cameroon. *Applied Earth Science*, 2017, 1743-2758.

[24] Ndema M.J.L. and Mbonjoh T.M.,. Assessment of Banded Iron Formations around Gouap Area asPotential High-Grade Iron Ore (Nyong Serie, Congo Craton -South Cameroon). *International Journal of Progressive Sciences and Technologies*, 22, 2020, 87-110.

[25] B. M. M. Bonda, Etame, J., Kouske, A. P., Bayiga, E. C., Ngon Ngon, G. F., Mbaï, S. J., Gérard, M., Ore Texture, Mineralogy and Whole Rock Geochemistry of the Iron Mineralization from Edea North Area, Nyong Complex, Southern Cameroon: Implication for Origin and Enrichment Process. *International Journal of Geosciences*, 8, 2017, 659-677.

[26] Toteu, S.F., Van Schmus, R.W., Penaye, J., Nyobe, J.B., U-Pb and Sm-Nd evidence for Eburnean and Pan-African high grade metamorphism in cratonic rocks of southern Cameroon. *Precambrian research*, 67, 1994, 321-347.

[27] Lerouge, C., Cocherie A., Toteu, S. F., Penaye, J., Milési J. P., Tchameni, R., Nsifa, E. N., Fanning, C. M., Deloule, E., Shrimp U–Pb zircon age evidence for Paleoproterozoic sedimentation and 2.05 Ga syntectonic plutonism in the Nyong Group, South-Western Cameroon: consequences for the Eburnean–Transamazonian belt of NE Brazil and Central Africa. *Journal of African Earth Sciences* 44, 2006, 413-427.

[28] Penaye, J., Toteu, S.F., Tchameni, R., Van Schmus, W.R., Tchakounté, J., Ganwa, A., Minyem, D., Nsifa, E.N., The 2.1Ga West Central African Belt in Cameroon: extension and evolution. *Journal of African Earth Sciences* 39, 2004, 159-164.

[29] Ndema Mbongue J. L., Ngnotue T., Ngo Nlend C. D., Nzenti J. P., Cheo Suh E., Origin and Evolution of the Formation of the Cameroon Nyong Series in the Western Border of the Congo Craton. *Journal of Geosciences and Geomatics*, Vol. 2, 2014, 62-75.

[30] Owona, S., Archaean, *Eburnean and Pan-African features and relationships in their junction zone in the South of Yaounde (Cameroon)*. Ph.D. Thesis. University of Douala, Cameroon, 2008, 232 p.

[31] Feybesse, J.L., Johan, V., Maurizot, P., Abessolo, A., Mise en évidence d'une nappe syn-métamorphe d'âge éburnéen dans lapartie Nord-Ouest du Craton zaïrois, Sud-Ouest Cameroun. In: Lesformations birrimiennes en Afrique de l'Ouest, journée scientifique, *compte rendu de conferences*. Occasional Publications CIFEG, 1986/10, 1986, pp. 105-111.

[32] Omang, O.B., *Stream sediment geochemistry and placer gold microchemical signature in Eastern and Southern Cameroon*. Ph.D. Thesis, University of Buea, Cameroon. Unpublished, 2015, 290 p.

[33] Maurizot, P., Abessolo, A., Feybesse, J.L., Johan, V., Lecomte, P., Etude et prospection minière du Sud-Ouest Cameroun. Synthèse des travaux de 1978 à 1985. *BRGM Report 85 CMR 066*, 1986.

[34] Marvine N.T., Sylvestre G., Olugbenga A.O., Evine L.T.N., Landry S.T., Brice K.W., Arnold S.M.M. and Jean P.N., Petrogenesis and tectonic setting of the Paleoproterozoic KelleBidjoka iron formations, Nyong group greenstone belts, southwestern Cameroon. Constraints from petrology, geochemistry, and LA-ICP-MS zircon U-Pb geochronology, *International Geology Review*, 2020.

[35] Rudnick, R. L., and Gao, S., Composition of the Continental Crust. *In: Holland, H.D.*, 2003.

[36] Duparc, Q., Dare, S. A.S., Cousineau, Pierre, A., Goutier, A., Magnetite chemistry as a provenance indicator in Archean metamorphosed sedimentary rocks. *Journal of Sedimentary Research 86*, 2016, 542-563.

[37] Dare, S.A.S., Barnes, S.J., Méric, J., Néron, A., Beaudoin, G., Boutroy, E., The use of trace elements in Fe-oxides as provenance and petrogenetic indicators in magmatic and hydrothermal environments. *Mineral Deposit Research For a High-Tech World, 12th SGA Biennial Meeting 2013*. Proceedings, Volume 1, 2014, 256-259.

[38] Canil D, Grondahl C, Lacourse T, Pisiak L.K., Trace elements in magnetite from porphyry Cu-Mo-Au deposits in British Columbia, Canada. *Ore Geology Reviews 72*, 2016, 1116-1128.

[39] Grigsby, J., Detrital magnetite as a provenance indicator. *Journal of Sedimentary Petrology 60*, 1990, 940-951.

[40] Zhen-Ju Z., Hao-Shu T., Yan-Jing C., Zheng-Le C., Trace elements of magnetite and iron isotopes of the Zankan iron deposit, westernmost Kunlun, China: A case study of seafloor hydrothermal iron deposits. *Ore Geology Reviews 80*, 2016, 1191-1205.

[41] Verlaguet, A., Brunet, F., Goffé, B., Murphy, W.M., Experimental study and modelling of fluid reaction paths in the quartz–kyanite ± muscovite–water system at 0.7 GPa in the 350-550°C range: implications for Al selective transfer during metamorphism. *Geochimical Cosmochimical Acta 70*, 2006, 1772-1788.

[42] Ndema M.J.L. and Mbonjoh T.M., Assessment of Banded Iron Formations around Gouap Area asPotential High-Grade Iron Ore (Nyong Series, Congo Craton -South Cameroon). *International Journal of Progressive Sciences and Technologies, 22*, 2020, 87-110.

[43] Gross, G. A. and Mcleod, C. R., A preliminary assessment of the chemical composition of iron formation in Canada. *Canadian Mineralogist 18*, 1980, 223-229.

[44] Armstrong, H. A., Owen, A. W., Floyd, J. D., Rare earth geochemistry of Arenig cherts from the Ballantrae Ophiolite and Leadhills Imbricate Zone, southern Scotland: implications for origin and significance to the Caledonian Orogeny. *Journal of of Geology Society 156 (3)*, 1999, 549-560.